Vector Rogue Waves and Baseband Modulation Instability in the Defocusing Regime

Fabio Baronio,[1,*] Matteo Conforti,[2] Antonio Degasperis,[3] Sara Lombardo,[4] Miguel Onorato,[5,6] and Stefan Wabnitz[1]
[1]Dipartimento di Ingegneria dell'Informazione, Università di Brescia, Via Branze 38, 25123 Brescia, Italy
[2]PhLAM/IRCICA UMR 8523/USR 3380, CNRS-Université Lille 1, F-59655 Villeneuve d'Ascq, France
[3]INFN, Dipartimento di Fisica, "Sapienza" Università di Roma, Piazzale Aldo Moro 2, 00185 Roma, Italy
[4]Department of Mathematics and Information Sciences, Northumbria University, Newcastle upon Tyne NE2 1XE, United Kingdom
[5]Dipartimento di Fisica, Università di Torino, Via Pietro Giuria, 10125 Torino, Italy
[6]INFN, Sezione di Torino, Via Pietro Giuria 1, 10125 Torino, Italy
(Received 15 March 2014; published 16 July 2014)

We report and discuss analytical solutions of the vector nonlinear Schrödinger equation that describe rogue waves in the defocusing regime. This family of solutions includes bright-dark and dark-dark rogue waves. The link between modulational instability (MI) and rogue waves is displayed by showing that only a peculiar kind of MI, namely baseband MI, can sustain rogue-wave formation. The existence of vector rogue waves in the defocusing regime is expected to be a crucial progress in explaining extreme waves in a variety of physical scenarios described by multicomponent systems, from oceanography to optics and plasma physics.

DOI: 10.1103/PhysRevLett.113.034101 PACS numbers: 05.45.Yv, 02.30.Ik, 42.65.Tg

Introduction.—Rogue waves are extremely violent phenomena in the ocean: an encounter with such a wave can be disastrous even to big ocean liners. These waves can also be very dangerous for various hydrotechnic constructions. This makes the study of rogue waves a very important problem. Hence, it is not surprising that the phenomenon of rogue waves has attracted ample attention of oceanographers in the last decade [1–4]. However, although the existence of rogue waves has now been confirmed by multiple observations, uncertainty remains on their fundamental origins. This hampers systematic approaches to study their characteristics, including the predictability of their appearance [5].

The research on rogue waves in oceans has attracted recently the attention of researchers in many other fields of physics [6]: optics [7], atmosphere [8], plasmas [9], and Bose-Einstein condensates [10].

The possibility to reach a general understanding of rogue-wave formation is still an open question [6]. Nonetheless, the ongoing debate stimulates the comparison of predictions and observations between distinct topical areas, in particular, hydrodynamics and nonlinear optics [11], in situations where analogous dynamical behaviors can be identified through the use of common mathematical models.

So far, the focusing nonlinear Schrödinger equation (NLSE) has played a pivotal role as a universal model for rogue-wave solutions. The Peregrine soliton, predicted 30 years ago [12], is the simplest rogue-wave solution associated with the focusing NLSE, and it has been recently experimentally observed in optical fibers [13], water-wave tanks [14], and plasmas [9].

While rogue-wave investigations are flourishing in several fields of science, moving beyond the standard focusing NLSE description in order to model more general and important classes of physical systems is both relevant and necessary. In this direction, recent developments consist in (i) including dissipative terms, since a substantial supply of energy (e.g., wind in oceanography) is generally required to drive rogue-wave formation [15], or in (ii) including higher-order perturbation terms such as in the Hirota equation and in the Sasa-Satsuma equation [16,17], because of the high amplitude or great steepness of a rogue wave, or in (iii) considering wave propagation in $2+1$ dimensions as for the Davey-Stewartson equation [18]. Additional important progress has been recently obtained by extending the search for rogue-wave solutions to coupled-wave systems, since numerous physical phenomena require modeling waves with two or more components in order to account for different modes, frequencies, or polarizations. When compared to scalar dynamical systems, vector systems may allow for energy transfer between their additional degrees of freedom, which potentially yields rich and significant new families of vector rogue-wave solutions. Indeed, rogue-wave families have been recently found as solutions of the focusing vector NLSE (VNLSE) [19–22], the three wave resonant interaction equations [23,24], the coupled Hirota equations [25], and the long-wave-short-wave resonance [26].

It is a well-established fact that, for the scalar NLSE, the focusing nonlinear regime is a prerequisite for the emergence of regular or random rogue waves (see, e.g., the discussion in [6]). To the contrary, in the scalar case the defocusing nonlinear regime does not allow for rogue-wave solutions, even of a dark nature. In coupled-wave systems, is the focusing regime still a prerequisite for the existence of rogue-wave solutions? Or it possible to find examples of rogue waves in defocusing regimes?

Additionally, what are the conditions under which modulation instability (MI) may produce an extreme wave

event? Indeed, it is generally recognized that MI is among the several mechanisms which generate rogue waves [12]. A rogue wave may be the result of MI, but not every kind of MI leads to rogue-wave generation [27–29].

In this Letter, we prove the existence of rogue-wave solutions of the VNLSE in the *defocusing* regime. We evince that MI is a necessary but not a sufficient condition for the existence of rogue waves. In fact, rogue waves can exist if and only if the MI gain band also contains the zero-frequency perturbation as a limiting case (baseband MI).

Defocusing VNLSE and rogue waves.—We consider the VNLSE (also known as the Manakov system) which we write in the following dimensionless form:

$$\begin{aligned} iE_t^{(1)} + E_{xx}^{(1)} - 2s(|E^{(1)}|^2 + |E^{(2)}|^2)E^{(1)} = 0, \\ iE_t^{(2)} + E_{xx}^{(2)} - 2s(|E^{(1)}|^2 + |E^{(2)}|^2)E^{(2)} = 0, \end{aligned} \tag{1}$$

where $E^{(1)}(x,t)$, $E^{(2)}(x,t)$ represent the wave envelopes and x, t are the transverse and longitudinal coordinates, respectively. Each subscripted variable in Eq. (1) stands for partial differentiation. It should be pointed out that the meaning of the dependent variables $E^{(1)}(x,t)$, $E^{(2)}(x,t)$ and of the coordinates x, t depends on the particular applicative context (e.g., nonlinear optics, water waves, plasma physics).

We have normalized Eq. (1) in a way such that $s = \pm 1$. Note that in the case $s = -1$, Eq. (1) refers to the focusing (or anomalous dispersion) regime; in the case $s = 1$, Eq. (1) refers to the defocusing (or normal dispersion) regime.

Like the scalar NLSE, the focusing VNLSE, Eq. (1), also possesses rogue-wave solitons [19–22]. Unlike the scalar case, and far from being obvious, we find that rational solutions of the defocusing VNLSE do indeed exist, with the property of representing amplitude peaks which are localized in both x and t coordinates. These solutions are constructed by means of the standard Darboux dressing method [30,31] and, for Eq. (1) with $s = 1$, they can be expressed as

$$E^{(j)} = E_0^{(j)} \left[\frac{p^2x^2 + p^4t^2 + px(\alpha_j + \beta\theta_j) - i\alpha_j p^2 t + \beta\theta_j}{p^2x^2 + p^4t^2 + \beta(px+1)} \right], \tag{2}$$

where

$$\begin{aligned} E_0^{(j)} = a_j e^{i(q_j x - \nu_j t)}, \qquad \nu_j = q_j^2 + 2(a_1^2 + a_2^2), \\ j = 1, 2, \end{aligned} \tag{3}$$

represent the backgrounds of Eq. (2),

$$\begin{aligned} \alpha_j &= 4p^2/(p^2 + 4q_j^2), \\ \theta_j &= (2q_j + ip)/(2q_j - ip), \qquad j = 1, 2; \\ \beta &= p^3/\chi(p^2 + 4q_1q_2), \qquad p = 2\mathrm{Im}(\lambda + k), \\ q_1 + q_2 &= 2\mathrm{Re}(\lambda + k), \qquad q_1 - q_2 = 2q, \qquad \chi = \mathrm{Im}k. \end{aligned}$$

As for the computation of the complex value of λ and k (see [24]), λ is the double solution of the polynomial:

$$\lambda^3 + A_2\lambda^2 + A_1\lambda + A_0 = 0, \tag{4}$$

with

$$\begin{aligned} A_0 &= -k^3 + k(q^2 + a_1^2 + a_2^2) + q(a_2^2 - a_1^2); \\ A_1 &= -k^2 - q^2 + a_1^2 + a_2^2; \\ A_2 &= k. \end{aligned}$$

The constraint on the double roots in Eq. (4) is satisfied when the discriminant of Eq. (4) is zero, which results in the fourth order polynomial condition:

$$k^4 + D_3k^3 + D_2k^2 + D_1k + D_0 = 0, \tag{5}$$

with

$$\begin{aligned} D_0 &= (q^2 - a_1^2 - a_2^2)^3/(2^4q^2) - (3/4)^3(a_2^2 - a_1^2)^2; \\ D_1 &= -9(a_2^2 - a_1^2)(2q^2 + a_1^2 + a_2^2)/(2^4q); \\ D_2 &= -[8q^4 - (a_1^2 + a_2^2)^2 + 20q^2(a_1^2 + a_2^2)]/(2^4q^2); \\ D_3 &= (a_2^2 - a_1^2)/(2q). \end{aligned}$$

Thus, λ is the double solution of the third order polynomial, Eq. (4), and k is either one of the strictly complex solutions of the fourth order polynomial, Eq. (5) [real solutions have to be neglected to avoid singular solutions in Eq. (2)].

The expressions reported above depend on the real parameters a_1, a_2 and q which originate from the naked solution, Eq. (3), namely, from the backgrounds: a_1, a_2 represent the amplitudes, and $2q$ represents the "frequency" difference of the waves.

Figure 1 shows a typical dark-bright solution, Eq. (2), while Fig. 2 shows a typical dark-dark solution, Eq. (2).

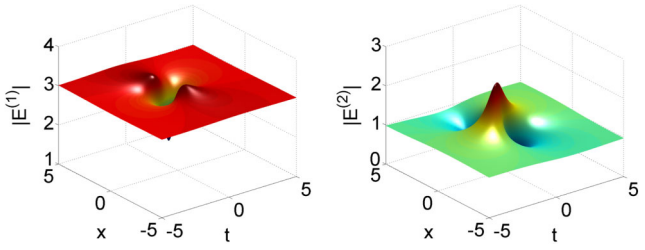

FIG. 1 (color online). Rogue waves envelope distributions $|E^{(1)}(x,t)|$ and $|E^{(2)}(x,t)|$ of Eq. (2). Here, $a_1 = 3, a_2 = 1$, $q = 1$. $k = 2.36954 + 1.1972i$ and $\lambda = -1.69162 - 1.79721i$.

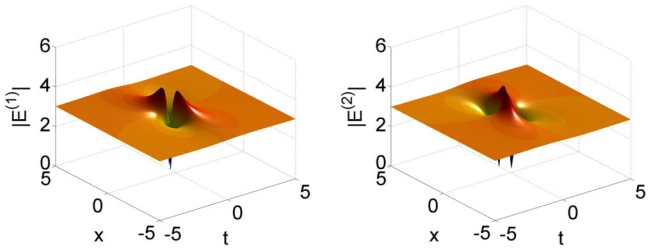

FIG. 2 (color online). Rogue waves envelope distributions $|E^{(1)}(x,t)|$ and $|E^{(2)}(x,t)|$ of Eq. (2). Here, $a_1 = 3, a_2 = 3$, $q = 1$. $k = 4.02518i$ and $\lambda = -4.92887i$.

The family of solutions, Eq. (2), found in the defocusing regime, possesses a novel feature with respect to families of the solutions of Eq. (1) previously reported in focusing regimes (see, e.g., [20–22]). In fact, in the defocusing regime, threshold conditions for the parameters a_1, a_2, q exist due to the requirement that the solution k of Eq. (5) must be strictly complex, and that λ is a double solution of Eq. (4). We have identified these threshold conditions by computing the discriminant of Eq. (5). If this discriminant is positive, Eq. (5) possesses four real k roots, and rogue waves do not exist, while if the discriminant is negative, Eq. (5) has two real roots, to which no rogue wave is associated, and two complex conjugate k roots, which instead imply the existence of rogue waves. This constraint on the sign of the discriminant leads to the following rogue-wave existence condition:

$$(a_1^2 + a_2^2)^3 - 12(a_1^4 - 7a_1^2a_2^2 + a_2^4)q^2 + 48(a_1^2 + a_2^2)q^4 - 64q^6 > 0. \quad (6)$$

Figures 3(a) and 3(b) report two characteristic examples of rogue-wave existence conditions. In particular, Fig. 3(b) shows that, for fixed q, the background amplitudes have to be sufficiently large to allow for rogue-wave formation. As a particularly simple example, consider the case $a_1 = a_2 = a$ and $q \neq 0$. In this case, the inequality, Eq. (6), reads $4(a^2 + 4q^2)^2(2a^2 - q^2) > 0$, with the implication that only in the (large amplitudes) subset $a^2 > q^2/2$ of the parameter plane (a, q) do the rogue waves, Eq. (2), exist.

Defocusing VNLSE and induced MI.—Here we first turn our attention to the standard linear stability analysis of the background solution, Eq. (3), and then we prove that the existence of rogue waves is strictly related with a specific form of MI, namely, to baseband MI. In the following, the coupling parameter s in Eq. (1) is considered as a continuous variable rather than a discrete, two-valued variable (i.e., $s = \pm 1$). Therefore, the background solution takes the expression $E_0^{(j)} = a_j e^{i(q_j x - \nu_j t)}$, with $\nu_j = q_j^2 + 2s(a_1^2 + a_2^2)$, $j = 1, 2$, while a_1, a_2 represent "amplitudes" (which, with no loss of generality, we take as real valued), and q_1, q_2 represent "frequencies." A perturbed nonlinear background can be written as $E_p^{(j)} = [a_j + p_j]e^{iq_j x - i\nu_j t}$, where $p_j(x,t)$ are small perturbations (in amplitude and phase) which satisfy a linear equation. Whenever $p_j(x,t)$ are x—periodic with frequency Q, i.e., $p_j(x,t) = \eta_{j,s}(t)e^{iQx} + \eta_{j,a}(t)e^{-iQx}$, their equations reduce to the 4×4 linear differential equation $\eta' = iM\eta$, with $\eta = [\eta_{1,s}, \eta_{1,a}^*, \eta_{2,s}, \eta_{2,a}^*]^T$ (here a prime stands for differentiation with respect to t). For any given real frequency Q, the generic perturbation $\eta(t)$ is a linear combination of exponentials $\exp(iw_j t)$ where $w_j, j = 1, \ldots, 4$, are the four eigenvalues of the matrix M. Since the entries M_{mn} of the matrix M are all real, $M_{11} = -Q^2 - 2Qq_1 - 2sa_1^2$, $M_{22} = Q^2 - 2Qq_1 + 2sa_1^2$, $M_{33} = -Q^2 - 2Qq_2 - 2sa_2^2$, $M_{44} = Q^2 - 2Qq_2 + 2sa_2^2$, $M_{12} = -M_{21} = -2sa_1^2$, $M_{13} = M_{14} = M_{31} = M_{32} = -M_{41} = -M_{23} = -M_{24} = -M_{42} = -2sa_1a_2$, $M_{43} = -M_{34} = 2sa_2^2$, the eigenvalues w_j are either real or come as complex conjugate pairs. They are the roots of the characteristic polynomial of the matrix M,

$$B(w) = w^4 + B_3 w^3 + B_2 w^2 + B_1 w + B_0, \quad (7)$$

with

$$B_0 = (Q^2 - 4q^2)[4(sa_1^2 + sa_2^2 - q^2) + Q^2]Q^4;$$
$$B_1 = 16q(sa_1^2 - sa_2^2)Q^3;$$
$$B_2 = -2[2(sa_1^2 + sa_2^2 + 2q^2) + Q^2]Q^2;$$
$$B_3 = 0.$$

Whenever M has an eigenvalue w with a negative imaginary part, $\mathrm{Im}\{w\} < 0$, MI exists (see [32–35] for details and review papers). Indeed, if the explosive rate is $G(Q) = -\mathrm{Im}\{w\} > 0$, perturbations grow exponentially like $\exp(Gt)$ at the expense of the pump waves. The bandwidth of MI $0 \leq Q_1 < Q < Q_2$ in which $G(Q) \neq 0$ is a baseband if $Q_1 = 0$ while it is a passband if $Q_1 > 0$.

MI is well depicted by displaying the gain $G(Q)$ as a function of s, a_1, a_2, q_1, q_2, and Q. Characteristic outcomes of the MI analysis are reported in Fig. 4.

Figure 4(a) corresponds to the case where the nonlinear background modes have the same frequencies ($q_1 = q_2$, thus $q = 0$). In this case, MI is always present in the focusing regime ($s < 0$), but it is absent in the defocusing regime ($s > 0$). This particular case corresponds to the trivial vector generalization of scalar NLSE MI dynamics.

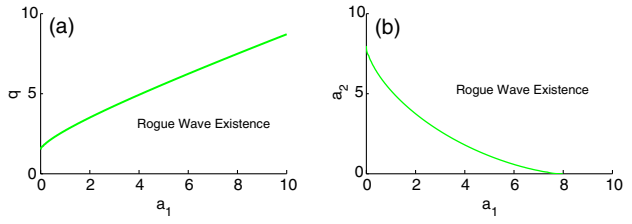

FIG. 3 (color online). Rogue-wave existence condition, Eq. (6). (a) (q, a_1) plane, with $a_2 = 3$. (b) (a_2, a_1) plane, with $q = 4$.

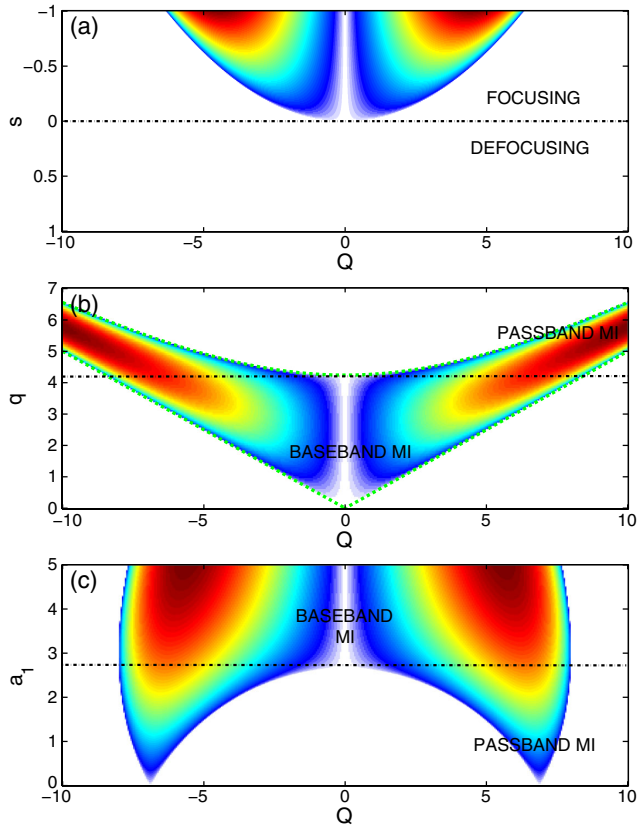

FIG. 4 (color online). Maps of MI of the VNLSE (1). (a) MI on the (Q, s) plane, calculated for the case $a_1 = 3, a_2 = 1$, $q_1 = q_2 = 1$. (b) MI on the (Q, q) plane, calculated for the case $a_1 = 3, a_2 = 3$, $q_1 = -q_2 = q$ and $s = 1$. Dotted (green) curves represent the analytical marginal stability condition $Q = 2q$, $Q^2 = \max\{4q^2 - 8a^2, 0\}$. (c) MI on the (Q, a_1) plane, calculated for the case $a_2 = 3, q_1 = -q_2 = 4$, and $s = 1$.

We remark that no rogue waves exist in this defocusing regime.

Figure 4(b) corresponds to the case where the nonlinear background modes have opposite frequencies ($q_1 = -q_2 = q$), in a defocusing regime $s = 1$ which yields MI. The higher that q is, the higher that G becomes. In the special case of equal background amplitudes $a_1 = a_2 = a$, the marginal stability conditions can be found analytically: $Q^2 = 4q^2$, $Q^2 = \max\{4q^2 - 8a^2, 0\}$. Thus, for $a^2 > q^2/2$, a baseband or low pass MI, which includes frequencies that are arbitrarily close to zero, is present (i.e., $0 < Q^2 < 4q^2$). Instead, for $a^2 \leq q^2/2$, the MI occurs for frequencies in the passband range $(4q^2 - 8a^2) < Q^2 < 4q^2$. We remark that in the previous section we have shown that rogue waves, Eq. (2), necessarily exist for $a^2 > q^2/2$ [e.g., the parameters of the rogue wave of Fig. 2 correspond to the baseband MI as shown in Fig. 4(b)]. Thus, rogue waves, Eq. (2), and baseband MI coexist.

Figure 4(c) corresponds to the case in which the nonlinear background modes have different frequencies ($q_1 = -q_2 = q$), and different input amplitudes $a_1 \neq a_2$ in the defocusing regime $s = 1$. For low values of a_1, only passband MI is present. By increasing a_1, the baseband MI condition is eventually reached.

Thus, we proceed by focusing our interest on the MI behavior in the limit $Q \to 0$, namely, on the occurrence of baseband MI. To this aim, we rewrite the characteristic polynomial (7) as $B(Qv) = Q^4 b(v)$ and consider the polynomial $b(v)$ at $Q = 0$, namely,

$$b(v) = v^4 + b_3 v^3 + b_2 v^2 + b_1 v + b_0, \tag{8}$$

with

$$b_0 = -16q^2(a_1^2 + a_2^2 - q^2);$$
$$b_1 = 16q(a_1^2 - a_2^2);$$
$$b_2 = -4(a_1^2 + a_2^2 + 2q^2);$$
$$b_3 = 0.$$

Next, we have evaluated the discriminant of Eq. (8). If the discriminant is positive, the polynomial, Eq. (8), possesses four real roots, and no MI occurs, while if the discriminant is negative, Eq. (8) possesses two real roots and two complex conjugate roots, and Eq. (1) exhibits baseband MI.

The interesting finding is that the previous sign constraint on the discriminant of the polynomial, Eq. (8), which leads to the baseband MI condition, turns out to coincide with the sign constraint, Eq. (6), which is required for rogue-wave existence.

These results are important as they show that (i) the rogue-wave solutions, Eq. (2), exist in defocusing regimes in the subset of the parameter space where MI is present, and (ii) the rogue-waves solutions, Eq. (2), exist if and only if baseband MI is present.

The link between baseband MI and rogue waves can be understood if we consider that these rogue waves are rational solutions; thus, when $t \to -\infty$, they approach the constant background plus weak long-term waves. The fact that these weak long waves eventually rise to a finite amplitude is basically equivalent to baseband instability. Our contribution has been that of substantiating this qualitative argument by precisely formulating the explicit condition for the existence of both the baseband MI and the rogue waves.

We verified the outcome of our theoretical analysis by numerically solving the VNLSE in a wide range of parameters. We found that in the baseband MI regime, multiple rogue waves are generated from noise on top of an unstable plane wave background. Whereas, in the case of passband MI, we observed the birth of nonlinear oscillations with a period corresponding to the peak gain MI frequency. Examples of nonlinear time evolutions are shown in the Supplemental Material [36].

Conclusions.—We presented and analyzed exact, explicit rogue-wave solutions of the defocusing VNLSE. This family of solutions includes both bright and dark components. Moreover, we clarified that the rogue-wave existence condition is strictly related to a very specific manifestation of MI, namely, MI whose bandwidth includes arbitrarily small frequencies.

Because of the widespread fundamental and applicative interest of the VNLSE in the defocusing regime (in hydrodynamics, it applies to the shallow water regime; in nonlinear optics it describes nonlinear materials with normal group velocity dispersion, or diffraction in materials with a negative nonlinearity), we believe that our extreme wave solutions may have a significant impact in a variety of physical situations.

The present research was supported by the Italian Ministry of University and Research (MIUR, Project No. 2009P3K72Z, Project No. 2012BFNWZ2), by the Italian Institute for Nuclear Physics (INFN Project No. RM41), by the Agence Nationale de la Recherche (ANR TOPWAVE), by the Netherlands Organisation for Scientific Research (NWO, Grant No. 639.031.622), and by ONR (Grant No. 214 N000141010991).

*Corresponding author.
fabio.baronio@unibs.it

[1] M. Hopkin, Nature (London) **430**, 492 (2004).
[2] P. Muller, C. Garret, and A. Osborne, Oceanography **18**, 66 (2005).
[3] S. Perkins, Science News **170**, 328 (2006).
[4] C. Kharif, E. Pelinovsky, and A. Slunyaev, *Rogue Waves in the Ocean* (Springer, Heidelberg, 2009).
[5] E. Pelinovsky and C. Kharif, *Extreme Ocean Waves* (Springer, Berlin, 2008).
[6] N. Akhmediev and E. Pelinovsky, Eur. Phys. J. Spec. Top. **185**, 1 (2010).
[7] M. Erkintalo, G. Genty, and J. M. Dudley, Opt. Lett. **34**, 2468 (2009); C. Bonatto, M. Feyereisen, S. Barland, M. Giudici, C. Masoller, J. R. Rios Leite, and J. R. Tredicce, Phys. Rev. Lett. **107**, 053901 (2011).
[8] L. Stenflo and P.-K. Shukla, J. Plasma Phys. **75**, 841 (2009).
[9] H. Bailung, S. K. Sharma, and Y. Nakamura, Phys. Rev. Lett. **107**, 255005 (2011).
[10] Y. V. Bludov, V. V. Konotop, and N. Akhmediev, Phys. Rev. A **80**, 033610 (2009).
[11] M. Onorato, S. Residori, U. Bortolozzo, A. Montina, and F. T. Arecchi, Phys. Rep. **528**, 47 (2013).
[12] D. H. Peregrine, J. Aust. Math. Soc. Series B, Appl. Math. **25**, 16 (1983).
[13] B. Kibler, J. Fatome, C. Finot, G. Millot, F. Dias, G. Genty, N. Akhmediev, and J. M. Dudley, Nat. Phys. **6**, 790 (2010).
[14] A. Chabchoub, N. P. Hoffmann, and N. Akhmediev, Phys. Rev. Lett. **106**, 204502 (2011).
[15] C. Lecaplain, Ph. Grelu, J. M. Soto-Crespo, and N. Akhmediev, Phys. Rev. Lett. **108**, 233901 (2012); M. Brunetti, N. Marchiandob, N. Berti, and J. Kasparian, Phys. Lett. A **378**, 1025 (2014).
[16] A. Ankiewicz, J. M. Soto-Crespo, and N. Akhmediev, Phys. Rev. E **81**, 046602 (2010).
[17] U. Bandelow and N. Akhmediev, Phys. Rev. E **86**, 026606 (2012).
[18] Y. Ohta and J. Yang, Phys. Rev. E **86**, 036604 (2012).
[19] B. L. Guo and L. M. Ling, Chin. Phys. Lett. **28**, 110202 (2011).
[20] F. Baronio, A. Degasperis, M. Conforti, and S. Wabnitz, Phys. Rev. Lett. **109**, 044102 (2012).
[21] L. C. Zhao and J. Liu, Phys. Rev. E **87**, 013201 (2013).
[22] B. G. Zhai, W. G. Zhang, X. L. Wang, and H. Q. Zhang, Nonlinear Anal. Real World Appl. **14**, 14 (2013).
[23] F. Baronio, M. Conforti, A. Degasperis, and S. Lombardo, Phys. Rev. Lett. **111**, 114101 (2013).
[24] A. Degasperis and S. Lombardo Phys. Rev. E **88**, 052914 (2013).
[25] S. Chen and L. Y. Song, Phys. Rev. E **87**, 032910 (2013).
[26] S. Chen, Ph. Grelu, and J. M. Soto-Crespo, Phys. Rev. E **89**, 011201(R) (2014).
[27] M. S. Ruderman, Eur. Phys. J. Spec. Top. **185**, 57 (2010).
[28] A. Sluniaev, Eur. Phys. J. Spec. Top. **185**, 67 (2010).
[29] C. Kharif and J. Touboul, Eur. Phys. J. Spec. Top. **185**, 159 (2010).
[30] The computation of rogue-wave solutions is based on the Darboux technique applied to the Lax pair associated with the VNLSE. This method is well known and does not need to be detailed here to any extent. The relevant literature is rather vast and we refer to [31] for the formalism and general set up adopted here, and to Refs. [20,24] (and to the literature quoted therein) for the basic arguments to follow for the construction of rational solutions.
[31] A. Degasperis and S. Lombardo, J. Phys. A **42**, 385206 (2009)
[32] J. E. Rothenberg, Phys. Rev. A **42**, 682 (1990).
[33] P. D. Drummond, T. A. B. Kennedy, J. M. Dudley, R. Leonhardt, and J. D. Harvey Opt. Commun. **78**, 137 (1990).
[34] E. Seve, P. Tchofo Dinda, G. Millot, M. Remoissenet, J. M. Bilbault, and M. Haelterman Phys. Rev. A **54**, 3519 (1996).
[35] J. Fatome, I. El-Mansouri, J. Blanchet, S. Pitois, G. Millot, S. Trillo, and S. Wabnitz J. Opt. Soc. Am. B **30**, 99 (2013).
[36] See Supplemental Material at http://link.aps.org/supplemental/10.1103/PhysRevLett.113.034101 for examples of nonlinear time evolutions of plane waves perturbed by small random noise in the baseband and passband MI regimes.